forests

MDPI

Article

GIS-Based Spatial Modeling of Soil Erosion and Wildfire Susceptibility Using VIIRS and Sentinel-2 Data: A Case Study of Šar Mountains National Park, Serbia

Uroš Durlević [1], Tanja Srejić [1], Aleksandar Valjarević [1,*], Bojana Aleksova [2], Vojislav Deđanski [1], Filip Vujović [3] and Tin Lukić [1,2]

[1] Faculty of Geography, University of Belgrade, Studentski Trg 3/3, 11000 Belgrade, Serbia; uros.durlevic@gef.bg.ac.rs (U.D.); tanja.srejic@gef.bg.ac.rs (T.S.); vojislav.dedjanski@gef.bg.ac.rs (V.D.); tin.lukic@dgt.uns.ac.rs (T.L.)
[2] Department of Geography, Tourism and Hotel Management, Faculty of Sciences, University of Novi Sad, Trg Dositeja Obradovića 3, 21000 Novi Sad, Serbia; aleksova_bojana@yahoo.com
[3] Department of Geography, Faculty of Philosophy, University of Montenegro, Danila Bojovića bb, 81400 Nikšić, Montenegro; vujovicfilip@hotmail.com
* Correspondence: aleksandar.valjarevic@gef.bg.ac.rs

Abstract: Soil erosion and wildfires are frequent natural disasters that threaten the environment. Identifying and zoning susceptible areas are crucial for the implementation of preventive measures. The Šar Mountains are a national park with rich biodiversity and various climate zones. Therefore, in addition to protecting the local population from natural disasters, special attention must be given to preserving plant and animal species and their habitats. The first step in this study involved collecting and organizing the data. The second step applied geographic information systems (GIS) and remote sensing (RS) to evaluate the intensity of erosion using the erosion potential model (EPM) and the wildfire susceptibility index (WSI). The EPM involved the analysis of four thematic maps, and a new index for wildfires was developed, incorporating nine natural and anthropogenic factors. This study introduces a novel approach by integrating the newly developed WSI with the EPM, offering a comprehensive framework for assessing dual natural hazards in a single region using advanced geospatial tools. The third step involved obtaining synthetic maps and comparing the final results with satellite images and field research. For the Šar Mountains (Serbia), high and very high susceptibility to wildfires was identified in 21.3% of the total area. Regarding soil erosion intensity, about 8.2% of the area is affected by intensive erosion, while excessive erosion is present in 2.2% of the study area. The synthetic hazard maps provide valuable insights into the dynamics of the erosive process and areas susceptible to wildfires. The final results can be useful for decision-makers, spatial planners, and emergency management services in implementing anti-erosion measures and improving forest management in the study area.

Keywords: forest management; natural hazards; forest monitoring; forest fires; remote sensing; forest ecology; environment; erosion potential model (EPM); wildfire susceptibility index (WSI); climate change

check for updates

Academic Editor: Chong Xu

Received: 5 February 2025
Revised: 23 February 2025
Accepted: 8 March 2025
Published: 10 March 2025

Citation: Durlević, U.; Srejić, T.; Valjarević, A.; Aleksova, B.; Deđanski, V.; Vujović, F.; Lukić, T. GIS-Based Spatial Modeling of Soil Erosion and Wildfire Susceptibility Using VIIRS and Sentinel-2 Data: A Case Study of Šar Mountains National Park, Serbia. *Forests* **2025**, *16*, 484. https://doi.org/10.3390/f16030484

1. Introduction

Global population growth, climate change, deforestation, and other natural and anthropogenic processes pose significant challenges for the modern world. As these processes intensify, various types of natural hazards occur more frequently and intensively [1,2]. Soil erosion and wildfires are among many countries' most common natural disasters [3,4].

Soil plays a fundamental role in Earth's critical zone [5], providing essential services such as supporting agricultural productivity, preserving biodiversity, and maintaining environmental quality—key contributors to achieving the United Nations Sustainable Development Goals (SDGs) [6]. Among various forms of land degradation, soil erosion is the most widespread [7]. This process can lead to significant consequences, including property damage, livelihood loss, diminished ecosystem services, and social and economic disruptions [8]. Recognized as a global issue [9], soil erosion poses a serious threat to agriculture and environmental sustainability worldwide [10]. The reduction in arable land due to soil erosion has raised concerns about the long-term sustainability of agriculture [11], with studies indicating a global decline in crop yields of about 0.4% annually [12].

Soil erosion also significantly impacts ecosystems, including the global carbon cycle [13], and is exacerbated by climate change through variations in rainfall, wind, and temperature patterns [14]. Wildfires, in particular, intensify soil erosion by removing vegetative cover and altering soil structure, thereby increasing runoff and sediment loss. Global warming has intensified soil erosion, particularly in semiarid regions, emphasizing the need for effective solutions [15]. Addressing soil erosion requires monitoring its processes, forms, and parameters across spatial and temporal scales, as changes in these factors influence erosion patterns and intensity [16,17].

Over the past few decades, various models have been developed to assess soil erosion intensity, with a steady increase in related research [9]. In this study, the erosion process's intensity was calculated using the erosion potential model (EPM), also known as the Gavrilović method [18]. Validation studies have demonstrated the EPM's high reliability and applicability in estimating soil erosion intensity [19,20].

Advancements in Earth observation technology and GIS tools have addressed many of the model's limitations, reducing subjectivity and enabling global applications [20–22]. These improvements have facilitated automated geospatial assessments, soil loss mapping, and predictions of erosion intensity under climate change scenarios [23–25]. Modifications to the original methodology have also expanded its applicability to diverse geographic conditions [26].

The effective conservation of natural values—such as biodiversity, geodiversity, and landscape diversity—requires a comprehensive assessment that includes evaluating the current in situ condition of these resources [27]. This is especially important considering that protected natural areas in Serbia are sensitive to various types of natural hazards [28–32]. This protection process becomes even more complex when areas with natural values are situated in border regions. The borders of Serbia are ecologically diverse, with some of the country's most sensitive biocenoses located in these areas [27]. This is particularly true for the Šar Mountains National Park. As the current state of protected areas in Serbia is well below the quantitative standards recommended by the EU, this study focuses on an area significantly larger than the current area of the Šar Mountains National Park. This area is one step closer to the realization of the "30 × 30" actions for a sustainable Europe (30% of the country's area to be protected by 2030). In this context, this study aims to assess fire and soil erosion hazard zones in the Šar Mountains. Wildfires, which are a subset of forest fires occurring in wildland areas, including forests, grasslands, and shrublands, cause significant ecological impacts, including soil erosion, changes in hydrology, increased greenhouse gas emissions, and contributions to global warming [33]. These effects destabilize ecosystems and threaten vital resources for human well-being [34].

Mapping wildfire vulnerability zones is essential for addressing the challenges posed by wildfires and developing effective management strategies. They pose significant ecological and socio-economic challenges, affecting forest composition and structure and creating environmental hazards with impacts on the atmosphere, infrastructure, and human well-being [35,36]. The interplay between wildfires and soil erosion amplifies these impacts, as a fire-induced loss of vegetation cover exacerbates erosion rates, further degrading landscapes and ecosystem services.

Geographic technologies like GIS are vital for wildfire detection and creating vulnerability maps, which provide crucial insights for evaluating wildfire conditions and supporting decision-making. However, simulating wildfire behavior using field data can be complex, which is why GIS models, maps, and databases are used for analysis [37]. Multi-criterion analysis methods, such as the analytic hierarchy process, supported by GIS tools, are widely used to assess fire risk by incorporating factors such as topography, climate, vegetation, and human impact [38].

Identifying the factors that contribute to fire-prone environments and understanding fire behavior are key to developing effective wildfire management plans [39].

The Mediterranean region has traditionally been the most vulnerable to wildfires in Europe [40], but recently, Central Europe has also seen an increase in fire activity [41]. Among European nations, Serbia has experienced a notable rise in fire incidents over the past two decades [42]. Forests cover approximately 27.200 km^2, or more than 31%, of the country's surface area [43]. During the observed period from 1990 to 2005, approximately 43.000 hectares of forest and forest land were destroyed due to the consequences of wildfires [30].

Significant changes in fire risk across Europe are projected for the transitional zone between the Mediterranean and Euro-Siberian regions [44], where the Balkan Peninsula is located. In this region, dominant oak and beech forests may be replaced by fire-prone evergreen Mediterranean vegetation [45], potentially exacerbating the risk of wildfires due to changes in vegetation type. Lukić et al. [3] noted an increase in the number of forest fires in Serbia between 2000 and 2012; however, the trend was not statistically significant.

This study aims to assess the fire vulnerability zones in the Šar Mountains using a GIS-based wildfire susceptibility index (WSI) methodology. Other approaches, including the analytic hierarchy process, logistic regression, and machine learning techniques such as random forest, have been widely used in wildfire risk assessments [46]. Numerous studies conducted globally have sought to identify fire-prone areas and evaluate wildfire risk, utilizing various methodologies. Among the approaches applied are the index-based method and AHP, each contributing valuable insights to the modeling of wildfire vulnerability [47,48]. The findings will inform the development of early warning systems, resource distribution, and fire management strategies to support sustainable land use and conservation efforts [49].

It is significant to note that the data and software utilized for wildfire vulnerability mapping, such as QGIS, are entirely open-source, making them widely accessible for research and practical applications [50,51]. Although historical records of wildfires and corresponding meteorological data are generally essential for a comprehensive assessment of wildfire risk, research emphasizes that effective wildfire vulnerability mapping can be conducted even in the absence of such specific datasets [52].

This investigation represents a significant advancement by integrating the EPM with a newly developed WSI within a GIS-RS framework to concurrently evaluate soil erosion and wildfire risks in the Šar Mountains—an area hitherto unexamined for these combined hazards—offering a comprehensive dual-hazard assessment applicable to data-limited regions. This approach uniquely links wildfire-induced erosion processes with soil vulnerability, providing a holistic understanding of their interconnected dynamics. Key objectives include (1) delineating areas of intensive and excessive soil erosion with emphasis on fire-affected zones; (2) formulating a new wildfire modeling methodology and zoning high-risk areas; (3) proposing protective measures for soil erosion and wildfires within the national park that account for their mutual reinforcement; and (4) quantifying correlations among influencing factors, including the role of wildfires as a driver of erosion.

These outcomes enhance the sustainable management of the protected area, supporting the adoption of protective measures that benefit decision-makers, local communities, and emergency management services. The primary contributions of this research lie in developing an integrated dual-hazard framework and delivering synthetic hazard maps that provide geospatial insights for the targeted mitigation of soil erosion and wildfire risks.

2. Materials and Methods

2.1. Study Area

The Šar Mountains (Šara) represent one of the largest mountain systems in Serbia. They are located in the far south of Serbia and partly includes the territory of North Macedonia [53]. The Šar Mountains were declared a national park in 1993 with an area of 228 km^2, while the permanent borders are planned to cover an area of 974 km^2 [54]. There are 77 settlements within the study area. The highest peak in Serbia, Velika Rudoka, lies in the Šara at 2660 m (Figure 1). The status of a national park was obtained due to its specific geographical features and rich biodiversity. Numerous landforms, such as glacial, periglacial, and high mountain vegetation, are represented. During the Pleistocene, the Šar Mountains had a snow line (2000 m), above which glaciers and glacial valleys formed. The Šar Mountains are one of the richest mountain systems in terms of water on the Balkan Peninsula.

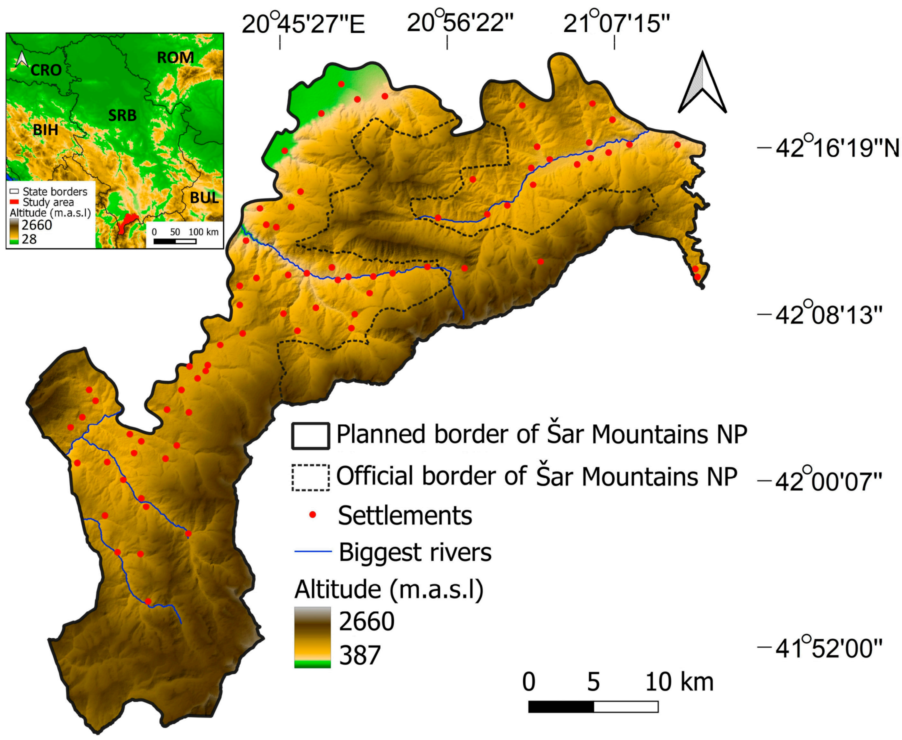

Figure 1. Geographical position of the Šar Mountains.

Climatically, this territory is characterized by three climates: Mediterranean, temperate, and alpine (Figure 2). The Mediterranean climate is represented in the northern part of the study area, the edge of the Prizren Basin. Here, summers are very warm, while winters are mild, often without snow cover. The Mediterranean influence comes from the Adriatic Sea, from the Bela Drim Valley to Prizren city, which makes this city the warmest in Serbia.

The temperate climate is represented in the largest part of the Šar Mountains. This territory has an altitude zone of 600–1700 m. The days are warm during the summer, while the nights are cool, so there is a large temperature oscillation. The winter is long and cold; from December to March, there is mainly snow cover. The alpine climate is characteristic of mountainous areas above 1700 m. In these areas, summers are short and sunny, while winters are extremely long and cold. Snow generally remains from December to May, while on the northern slopes, it often remains until August [55]. A great wealth of flora and fauna has developed at the contact of the three climates.

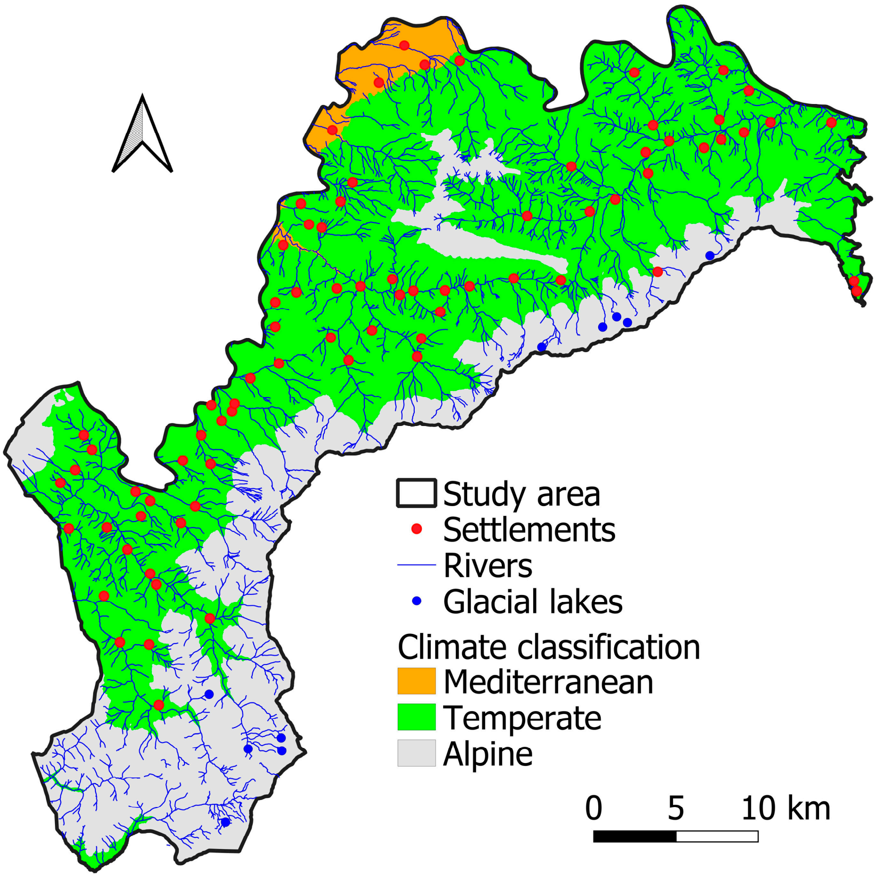

Figure 2. Hydro-climatic map of the Šar Mountains.

From the aspect of biodiversity, the study area is home to over 1800 plant species, many of which are local endemics and tertiary relicts: *Achillea alexandriregis*, *Bornmullera dieckii*, *Dianthus scardicus*, *Crocus scardicus*, *Verbascum scardicolum*, *Cerastium neoscardicum*, *Potentilla doerfleri*, *Hieracium scardicolum*, *Pinus heldreichii*, *Pinus peuce*, *Rhododendron ferrugineum*, etc. [56].

The national park is home to about 150 species of butterflies, 45 species of amphibians and reptiles, 200 species of birds, and 32 species of mammals, making the Šar Mountains one of Europe's most important faunal areas [56]. The forest area covers an area of 432 km^2, or 44.3% of the total territory [57].

Natural and anthropogenic factors influence the occurrence of the erosion process, while humans are responsible for the occurrence of wildfires in most cases (Figure 3) [29,58].

Figure 3. Soil erosion and wildfires in the Šar Mountains.

2.2. Data Sets and Criteria

Lithology: Depending on their granulometric composition, rock types have different effects on erosion. Sands, gravel, and other loose soil types are most susceptible to strong erosion. Alluvial soils and compact igneous rocks are exceptionally resistant and, as such, have the lowest coefficient for estimating erosion intensity [59]. Lithology data were obtained by digitizing the 1:100,000 basic geological map [60]. After that, the content was converted into a raster format with a spatial resolution of 12.5 m using QGIS software, where coefficients were assigned to each of the 16 rock types [50].

Land use: The degree of soil erosion largely depends on the vegetation types. Areas without vegetation cover (bare areas), arable land, and vineyards represent territories where the erosion process is significantly more intense, unlike meadows or well-structured forests that absorb a large amount of water on the surface [4]. From the aspect of wildfires, the evaluation is generally the opposite. The highest vulnerability coefficient is assigned to forests and shrub vegetation, while arable land and bare areas have the lowest fire risk [52]. Land use data were taken from the Environmental Systems Research Institute geoportal [61]. The classification was based on Sentinel-2 satellite images with a spatial resolution of 10 m.

Terrain slope: This is the most important geomorphological factor for assessing erosion intensity. Flat or relatively flat terrains are conducive to preventing the surface layer of soil from being eroded [62]. With increasing slope, there is an increase in the erosion power of plots [63]. The same approach is used when it comes to wildfires. Due to the increase in the slope of the terrain, grasslands and forest complexes burn faster than flat areas [64]. The data were obtained by processing a digital elevation model (DEM) with a spatial resolution of 12.5 m [65].

Bare-soil index (BSI): This is very applicable index for geospatial analyses concerning natural processes and phenomena [66]. For the purpose of the research, satellite images of the Sentinel-2 mission from August 2024, with a resolution of 10 m and 0% cloud cover, were used. The index was obtained using the following formula [67]:

$$BSI = \frac{(SWIR + RED) - (NIR + BLUE)}{(SWIR + RED) + (NIR + BLUE)}, \quad (1)$$

where SWIR is the shortwave infrared spectral band; RED is the red spectral band; NIR is the near-infrared spectral band; and BLUE is the blue spectral channel. The highest values of the index indicate the dominant presence of anthropogenic (settlements, roads) and bare surfaces, while the lowest values indicate forests [67]. In Figure 4, the GIS models of the criteria and datasets used for assessing soil erosion are presented.

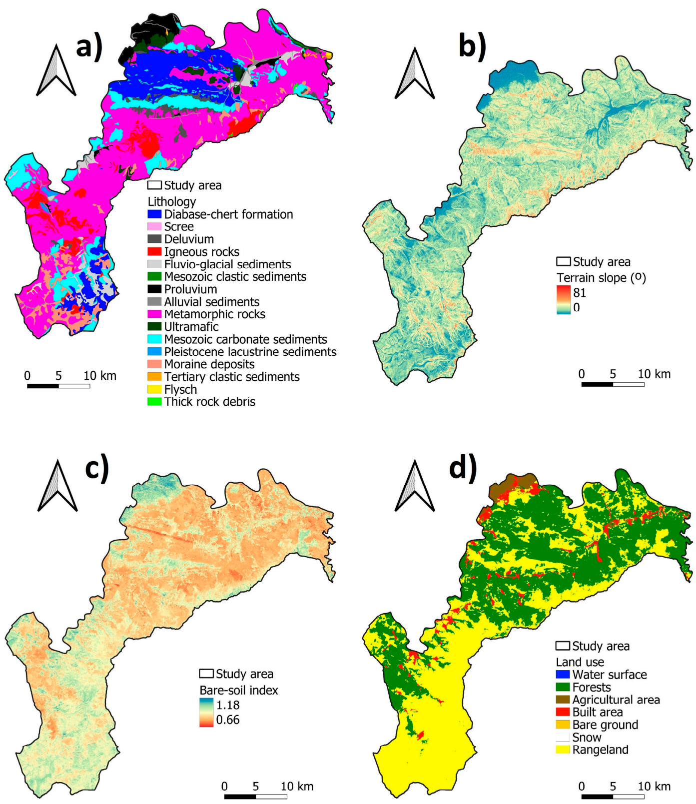

Figure 4. Analyzed criteria for assessing soil erosion: (**a**) lithology; (**b**) terrain slope; (**c**) bare-soil index; (**d**) land use.

Aspect: A morphometric condition that determines the degree of vulnerability to wildfires. South-facing areas are most susceptible due to a large number of sunshine hours. In contrast, north-facing areas are the least susceptible to fires due to less insolation, low temperatures, and higher humidity [68]. The aspect was obtained by reclassifying the DEM (12.5 m) in QGIS software [65].

Air temperature: Due to the significant difference in altitude within the study area, there are significant variations in air temperature throughout the year. The average annual temperature is −0.07 °C in the highest parts of the Šar Mountains, while in the valleys and lowlands, it is 11.7 °C. Increased air temperature increases the risk of fires [69]. However, this does not mean that fires will not occur during the winter. Due to climate change and increasing temperatures, in settlements at lower altitudes during the absence of snow and temperatures around 0 °C, fires often occur, the cause of which is anthropogenic activity [70]. The average air temperature was obtained by linear regression of data from three meteorological stations, Prizren (402 m), Brezovica (911 m), and Dragaš (1060 m), for the observed period of 1960–1988 [57]. The spatial resolution of the pixels was 12.5 m.

Precipitation: In the Šar Mountains, precipitation varies from 809 mm (valleys) to 1439 mm on the highest mountain peaks. The chances of fire occurrence are lower in locations that receive a large amount of precipitation [69]. The average winter precipitation was obtained by linear regression of data from five meteorological stations, Rečane (580 m), Štrpce (860 m), Jažince (950 m), Zaplužje (1160 m), and Restelica (1550 m), for the observed period 1960–1985 [57]. The spatial resolution of these pixels was 12.5 m.

Wind exposure: This one of the most important climatic factors. Windward slopes are characterized by higher air humidity, while leeward slopes are drier and, therefore, more susceptible to wildfires [71,72]. Data on wind exposure at a resolution of 12.5 m were obtained by processing DEM.

Distance from settlements: Since human activities cause the majority of fires, the distance from settlements is an important criterion for vulnerability analysis. Territories near settlements are much more vulnerable than inaccessible locations [73]. In the case study, the distance varies from 0 to 8913 m. The settlement data were first obtained by digitizing the objects in QGIS from the Google Satellite platform and then converted to raster format. The pixel resolution was 12.5 m (Figure 5).

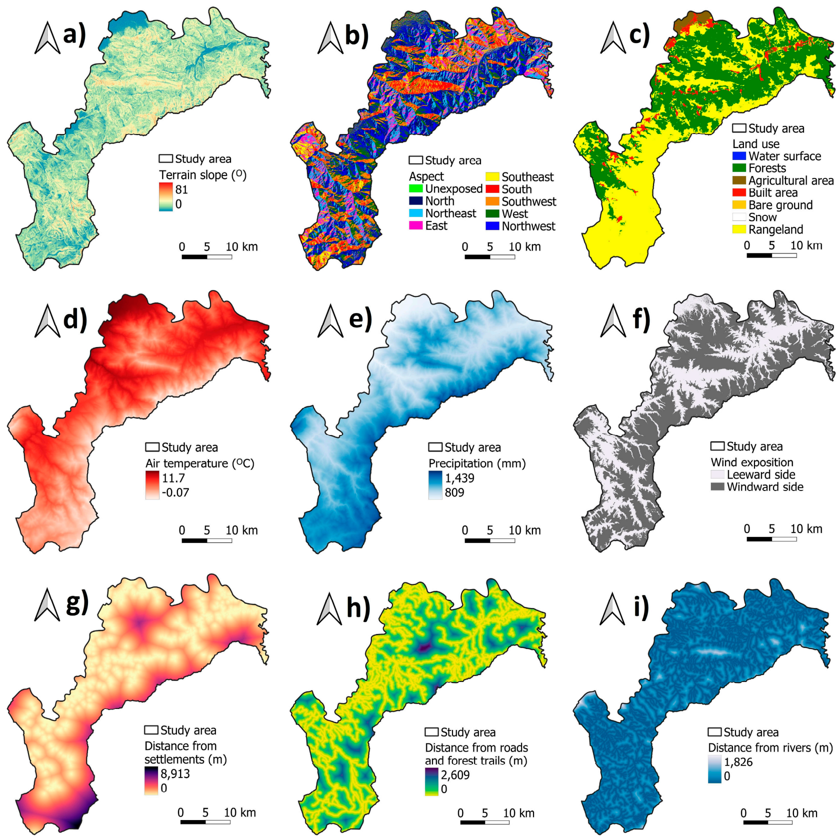

Figure 5. Analyzed criteria for assessing wildfires: (**a**) terrain slope; (**b**) aspect; (**c**) land use; (**d**) average annual air temperature; (**e**) precipitation; (**f**) wind exposure; (**g**) distance from settlements; (**h**) distance from roads and forest trails; (**i**) distance from rivers.

Distance from roads and forest trails: One possible cause of a fire is throwing cigarettes from a car into the natural environment. Another example is lighting a campfire in the forest next to paths. The closer a person is to a road or forest path, the greater the chances of a fire [74]. In the Šar Mountains, the distance varies from 0 to 2609 m. The data were obtained by digitizing all roads and forest trails using the QGIS software on the Open Street Map platform [75]. The vector content was converted to a raster with a resolution of 12.5 m.

Distance from rivers: When spatially analyzing endangered zones, it is necessary to include the hydrological factor. Due to higher humidity and lower air temperature, locations directly close to rivers are less vulnerable than those much further from river flows [76]. Within the study area, the distance ranges from 0 to 1826 m. River data were obtained by digitizing all rivers and streams in GIS software using the Open Street Map (2024) platform [75]. The entire content was converted to a raster with a resolution of 12.5 m.

2.3. Methodology

2.3.1. Erosion Potential Model (EPM)

Recent years have seen a growing number of studies around the world using the EPM to assess soil erosion risk on various scales [77–79], from large spatial units [19,80,81] to smaller areas [82–84], such as municipalities and settlements [29,38,85]. However, most studies focus on river basins as the primary spatial unit for analysis [4,86,87]. The erosion coefficient (Z) is calculated as follows:

$$Z = Y \cdot X \cdot \left(\varphi + \sqrt{I}\right), \tag{2}$$

where Y—coefficient of soil resistance, X—soil protection coefficient, φ—erosion and stream network development coefficient, and I—average slope (%). According to the research objectives set in this paper, the intensity of erosion will be considered using the Z coefficient [18].

The EPM uses a scoring approach for variables to calculate the coefficient of erosion (Table 1): the coefficient of soil resistance–lithology (Y), the coefficient of soil protection–land use (X), the coefficient of the type and extent of erosion–bare-soil index (ϕ), and the terrain slope (I).

Each sub-indicator has its own score. Values of 0 indicate very weak erosion, while the highest values indicate intensive and excessive erosion.

From a lithological point of view, scree, deluvium, and alluvial sediments (grade 2) were distinguished and given the highest rating because they represent unbound sediments that are very susceptible to erosion due to weak cohesion between particles of unbound sedimentary rocks.

Regarding land use, the highest rating was given to bare soil (1) and agricultural areas (0.85) due to the significantly disturbed surface and pedological layer. In such conditions, the soil is weakly bound to the geological base and susceptible to more intensive leaching.

The bare-soil index was obtained by processing satellite images and indicates the degree of soil bareness. In this case, the highest values (1.21) indicate a completely bare pedological cover that is extremely vulnerable to excessive erosion.

The slope of the terrain determines the rate of runoff of eroded soil. As the slope of the terrain increases, the rate and erosive potential of runoff increase [88,89]. The average terrain slope is obtained from the 25 m digital elevation model (DEM) as a percentage expressed in decimal notations. The highest values (5.96%) indicate the steepest terrain in the Šar Mountains.

Table 1. Evaluation of EPM criteria.

Criteria	Parameter	Grade	Area (km^2)	Share in Total Area (%)
Lithology	Diabase–chert formation	0.25	134.94	13.86
	Scree	2	1.74	0.18
	Deluvium	2	26.01	2.67
	Igneous rocks	0.2	60.91	6.26
	Fluvio-glacial sediments	1.8	29.94	3.07
	Mesozoic clastic sediments	1.8	1.79	0.18
	Proluvium	1.9	30.35	3.12
	Alluvial sediments	2	16.02	1.65
	Metamorphic rocks	0.9	465.23	47.78
	Ultramafic	0.35	25.39	2.61
	Mesozoic carbonate sediments	0.35	125.11	12.85
	Pleistocene lacustrine sediments	1.9	3.00	0.31
	Moraine deposits	1.8	49.95	5.13
	Tertiary clastic sediments	0.9	1.93	0.20
	Flysch	0.9	0.54	0.05
	Thick rock debris	0.2	0.87	0.09
Land use	Water surface	0	0.03	0.003
	Forests	0.25	431.78	44.34
	Agricultural areas	0.85	18.09	1.86
	Built area	0.05	36.23	3.72
	Bare ground	1	0.06	0.006
	Snow	0.3	0.02	0.002
	Rangeland	0.3	487.51	50.07
Bare-soil index	(BSI + 1)	From 0.67 to 1.21	Overall	100%
Terrain slope	Decimal slope	From 0 to 5.96	Overall	100%

2.3.2. Wildfire Susceptibility Index (WSI)

Based on a review and analysis of previous studies on wildfires, a new index—the wildfire susceptibility index (WSI)—was developed, incorporating all necessary criteria that can be obtained from open data. A team of experts in environmental science, forest management, climate change, and hydrology identified nine criteria: land use, terrain slope, aspect, wind, precipitation, air temperature, distance from rivers, distance from roads and forest trails, and distance from settlements. Equal importance or a weighting coefficient was assigned to each criterion.

The WSI is calculated using the following formula:

$$\mathrm{WSI} = \frac{\mathrm{TS} + \mathrm{A} + \mathrm{LU} + \mathrm{AT} + \mathrm{P} + \mathrm{WE} + \mathrm{DS} + \mathrm{DFR} + \mathrm{DR}}{9}, \quad (3)$$

where TS—terrain slope; A—aspect; LU—land use; AT—air temperature; P—precipitation; WE—wind exposure; DS—distance from settlements; DFR—distance from roads and forest trails; and DR—distance from rivers.

Each criterion can have values from 0 to 1. A value of 0 indicates the impossibility of fire occurrence, while a value of 1 indicates a very high degree of wildfire hazard (Table 2).

A hazard map is obtained by overlapping and multiplying all values within the criteria, where the final score interval varies from 0 to 1. To qualitatively determine the degree of vulnerability, the values in the synthesized map are reclassified into five classes: very low (0–0.4), low (0.4–0.55), medium (0.55–0.7), high (0.7–0.8), and very high (0.8–1) susceptibility. These thresholds were assigned based on field research in susceptible areas and visual analysis of the results obtained through GIS software. All forest fires are classified as wildfires, so the WSI is applicable to forest ecosystems, meadows, pastures, and other types of low vegetation.

Table 2. Evaluation of WSI criteria.

Criteria	Parameter	Grade	Area (km^2)	Share in Total Area (%)
Terrain slope (°)	0–4	0.2	40.39	4.14
	4–8	0.4	67.75	6.95
	8–12	0.6	111.67	11.46
	12–16	0.8	155.83	15.99
	>16	1	599.05	61.46
Aspect	Unexposed	0.9	3.28	0.34
	North	0.1	163.47	16.79
	Northeast	0.2	133.98	13.76
	East	0.4	90.27	9.27
	Southeast	0.8	74.59	7.66
	South	1	90.21	9.26
	Southwest	0.9	113.26	11.63
	West	0.5	140.31	14.41
	Northwest	0.3	164.36	16.88
Land use	Water surface	0	0.03	0.003
	Forests	1	431.78	44.34
	Agricultural areas	0.6	18.09	1.86
	Built area	0.2	36.23	3.72
	Bare ground	0.1	0.06	0.006
	Snow	0	0.02	0.002
	Rangeland	0.9	487.51	50.07
Air temperature (°C)	<2.34	0.2	50.71	5.21
	2.34–4.68	0.4	222.30	22.83
	4.68–7	0.6	295.21	30.32
	7–9.36	0.8	310.40	31.88
	>9.36	1	95.02	9.76
Precipitation (mm)	<934	1	48.21	4.95
	934–1060	0.8	222.06	22.81
	1060–1186	0.6	300.22	30.83
	1186–1312	0.4	308.97	31.73
	>1312	0.2	94.18	9.67
Wind exposure	Windward	0.5	583.03	59.88
	Leeward	1	390.62	40.12
Distance from settlements (m)	0–50	1	38.52	3.96
	50–150	0.8	50.88	5.23
	150–300	0.6	69.44	7.13
	300–500	0.4	90.34	9.28
	>500	0.2	724.54	74.41
Distance from roads and forest trails (m)	0–100	1	203.06	20.85
	100–300	0.8	254.67	26.15
	300–500	0.6	168.15	17.27
	500–700	0.4	115.67	11.88
	>700	0.2	232.18	23.84
Distance from rivers (m)	0–50	0.2	156.26	16.05
	50–200	0.4	362.58	37.24
	200–350	0.6	226.54	23.27
	350–500	0.8	119.05	12.23
	>500	1	109.30	11.22

With increasing terrain slope, wildfires are more likely due to drier vegetation on steep slopes and lower soil moisture. Due to the intense solar radiation on southern exposures, vegetation is significantly warmer and drier than that of other flora in other exposures. From the perspective of land use, forests are highly susceptible to fires due to dense vegetation that ignites easily. Higher air temperatures, lower precipitation, and leeward sides represent important climatic determinants under which vegetation becomes drier and more susceptible to fire. A smaller distance of the area from roads and settlements indicates greater anthropogenic activities, thus increasing the risk of fires caused by human activity. From a hydrological perspective, the humidity of territories far from rivers is much lower, so these terrains are drier and more susceptible to fires.

The WSI was developed using easily available data and a simple formula. The wildfire inventory obtained from the VIIRS (Visible Infrared Imaging Radiometer Suite) satellite instrument validated the final data. The VIIRS processes visible and infrared images and makes global observations of land, water, and the atmosphere. The data's spatial resolution is 375 m. The satellite data were downloaded from NASA's FIRMS (Fire Information for Resource Management System) platform [90].

All procedures and approaches employed in this research are outlined in the flow chart provided in Figure 6.

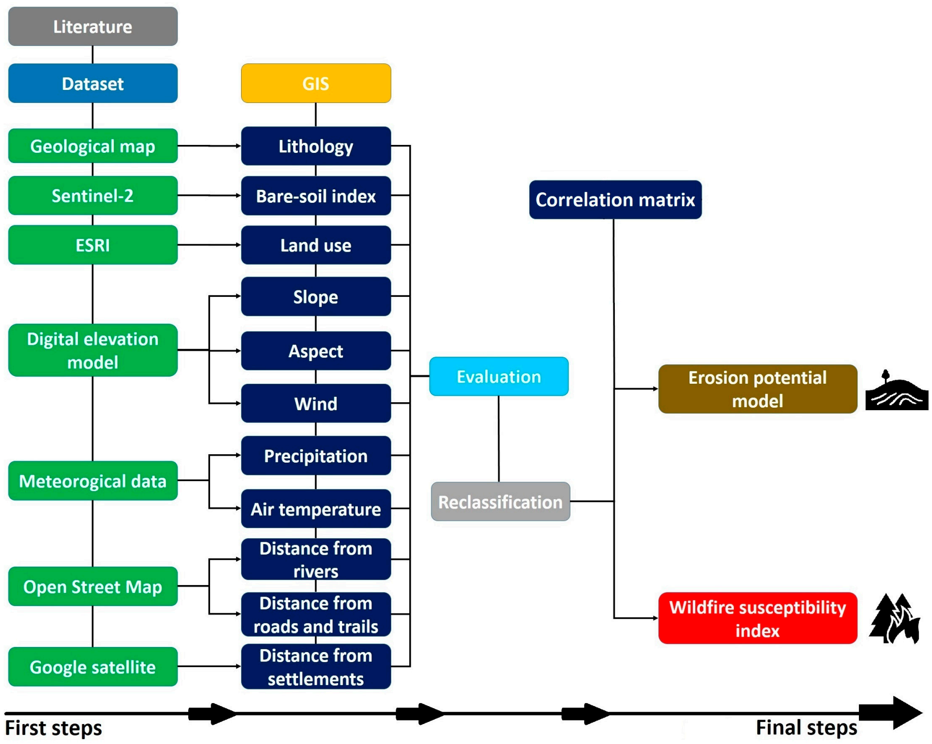

Figure 6. Flow chart with all the procedures and methods used in this research.

3. Results

3.1. Spatial Analysis of Erosion Intensity and Wildfire Susceptibility

By processing thematic maps in a GIS environment, synthetic maps of soil erosion and wildfire vulnerability were generated. The results of the EPM model indicated that the average erosion coefficient in 2024 was Z = 0.355, classifying the study area as having weak erosion—category IV (Z = 0.21–0.40). According to Table 3, 374.57 km^2 (38.49%) of the study area was classified as exhibiting very weak erosion. Over one-third of the total area (35.65%) was affected by weak erosion. The results also show that 149.81 km^2 (15.40%) was classified as medium erosion. Finally, intensive erosion covered 80.61 km^2 (8.28%), while excessive erosion affected 21.16 km^2 (2.17%).

Table 3. Susceptibility of the terrain to soil erosion and wildfires.

Erosion Intensity	Area (km^2)	Share of Total Area (%)	Wildfire Susceptibility	Area (km^2)	Share of Total Area (%)
Very weak	374.57	38.49	Very low	1.82	0.19
Weak	346.93	35.65	Low	204.89	21.06
Medium	149.81	15.40	Medium	558.65	57.41
Intensive	80.61	8.28	High	165.17	16.97
Excessive	21.16	2.17	Very high	42.53	4.37

Intensive and excessive erosion occurs in agricultural areas, bare ground, and areas with specific geological substrates (scree, deluvium, alluvial sediments). Bare soils on slopes are characterized by intense erosion, and the geological substrates include scree, deluvium, Mesozoic clastic sediments, proluvium, alluvial sediments, moraine deposits, and Tertiary clastic sediments.

The excessive type of erosion is spatially represented in the northern (edge of the Prizren Valley) and eastern parts (Sirinić Valley) of the study area (Figure 7). In these locations, arable land is represented at a certain slope, and proluvium and alluvial sediments dominate the geological substrate. In high-altitude areas, excessive erosion is represented by scree slopes under steep terrain. Settlements that are partially or wholly susceptible to intense or excessive erosion are Koriša, Grejkovce, Selogražde, Bogosovce, agricultural plots in the vicinity of the settlements of Berevece, Gotovuša, Drajkovce, Firaja, Koštanjevo, Dragaš, Brod, Restelica, Vranište, the Brezovica ski center, and the slopes above the settlement of Prevalac. It is necessary to establish specific protection measures at these locations. Contour tillage, terracing slopes, and the construction of anti-erosion belts should be considered for agricultural plots threatened by erosion [82]. In mountainous areas, intensive and excessive types of erosion should be mitigated through biological (afforestation) and technical (construction of transverse structures) means [91].

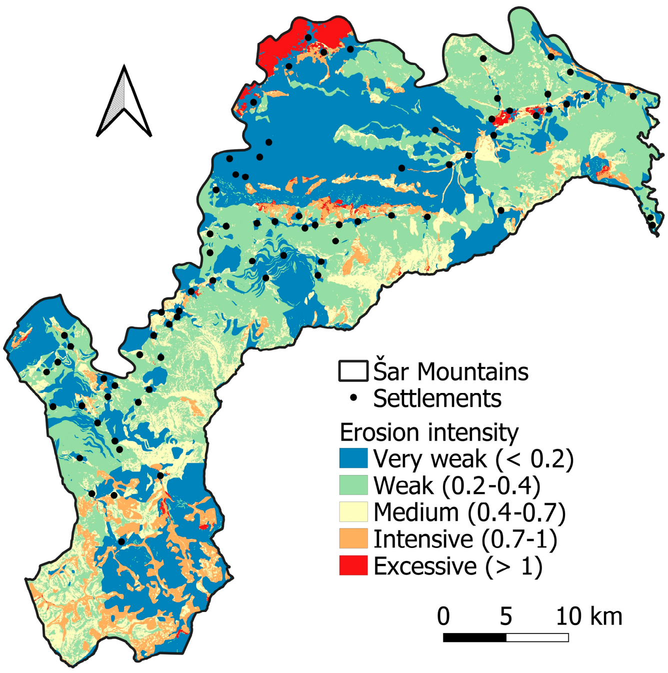

Figure 7. Map of erosion intensity (Z) in the Šar Mountains. Legend: very weak erosion—category V (Z = 0.01–0.20); weak erosion—category IV (Z = 0.21–0.40); medium erosion—category III (Z = 0.41–0.70); intensive erosion—category II (Z = 0.71–1.00); excessive erosion—category I (Z > 1.01).

The susceptibility to wildfires is generally higher near settlements. A very low degree is represented in only 0.19% of the area, and these are mountainous terrains facing north, with higher precipitation and very low air temperatures. About a fifth of the total territory (21%) exhibits a low level of vulnerability, which is also predominantly covered by mountainous, windward areas with low vegetation and greater distance from settlements and roads. The largest share of the area (57.41%) belongs to the medium class, which is characteristic of terrains between mountain peaks and valley bottoms. High (16.97%) and very high (4.37%) vulnerability dominates on leeward terrains exposed to the south, where higher air temperatures and lower precipitation occur (Figure 8).

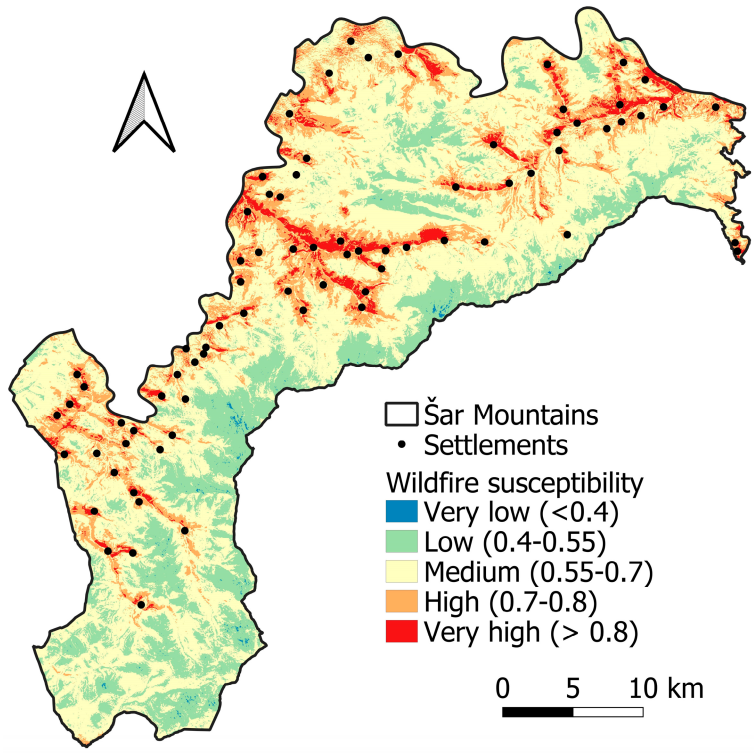

Figure 8. Map of wildfire susceptibility in the Šar Mountains.

These locations are also characterized by dense vegetation (forests) and relatively steep slopes and are near roads and settlements. When the results are compared with field research, it can be concluded that WSI is a very accurate and reliable method. In 2024, three wildfires occurred in the settlements of Drajkovce, Gornja Bitinja, and Prevalac. When these locations are overlapped with the synthesis map, they completely belong to the fourth and fifth categories (high and very high susceptibility).

Settlements that are partially or completely susceptible to wildfires are Gornje Selo, Prevalac, Vrbeštica, Brezovica ski center, Sevce, Berevce, Sušiće, Gornja Bitinja, Donja Bitinja, Viča, Ižance, Slatina, Globočica, Restelica, Zlipotok, Kruševo, Dikance, Bačka, Orćuša, Krstac, Dragaš, Zrze, Buzec, Kuklibeg, Pousko, Grnčar, Novo Selo, Manastirica, Gornje Ljubinje, Donje Ljubinje, Nebregošte, Rečane, Sredska, Drajčići, and Bogošovce. In all settlements belonging to the fourth or fifth class, it is necessary to install forest fire detection devices [30]. By doing so, emergency management services and protected area managers will have more time to take all measures to protect the local population and biodiversity.

3.2. Determination of Control Indicators–The Impact of Selected Criteria

In order to quantify the degree of dependence between the input parameters and soil erosion and to determine which of them best determines the soil erosion process in the study area, the correlation coefficient (r) between erosion intensity (Z) and all parameters individually was calculated. The first step in this procedure was to divide the study area using a grid. The basic spatial unit was a 2 km × 2 km square, quantitatively defined by the average value of each input parameter. The same procedure was applied to ensure wildfire susceptibility. The results of this mathematical interaction are shown in Figures 9 and 10. The results generally show a high correlation between the indicators at the significance level of $\alpha = 0.05$.

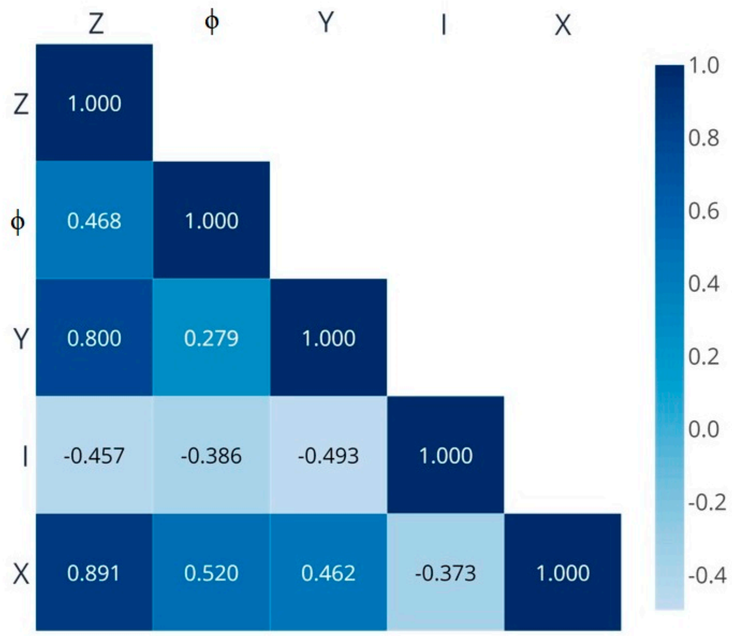

Figure 9. Correlation matrix (Pearson (r)) for parameters of the EPM for the calculation of erosion intensity (Z coefficient) in the Šar Mountains (significance level $\alpha < 0.0001$).

According to Figure 9, the correlation matrix at the level of statistical significance of $\alpha < 0.0001$ for the function Z = f (φ, Y, X, I) showed that almost all input parameters of the EPM have a significant impact on the intensity of soil erosion. Of the four variables that determine erosion, the coefficient of soil protection (X) is the primary factor controlling erosion intensity (r = 0.891). This is in line with the results of other studies [4,86]. The land use type is determined by φ (r = 0.520) and Y (r = 0.462). The second most important factor is the type of rock since the function Z = f(Y) is determined by a very high correlation coefficient (r = 0.800). A slightly weaker positive correlation (r = 0.468) is present in the function Z = f(φ). According to the mathematical interaction between the slope angle and other parameters, the correlation coefficients for the functions I = f(Z), I = f(φ), I = f (Y), and I = f (X) are r = −0.457, r = −0.386, r = −0.493, and r = −0.373, respectively. The negative correlation shows that erosion decreases with an increasing slope angle over most of this area. This is a direct consequence of the large share of forest cover and pastures (95%) located at higher altitudes and terrains with higher slope angles. Accordingly, the parameters X and φ decrease, and the share of erosion-resistant rocks increases. At the same time, this means that more erodible rocks are positioned on gentler terrain.

According to Figure 10, the correlation matrix for the function WSI = f (TS, A, LU, AT, P, WE, DS, DFR, DR) showed that air temperature and precipitation exert the greatest influence on WSI. The law of changes in precipitation and air temperature with altitude was also applied in this analysis. This law determined the relationship of these climate indicators with all other parameters. In this context, an almost identical relationship was identified between WSI and climate indicators (r = ±0.870). This means that parts of the study area with higher air temperatures and lower precipitation are more susceptible to fires. The quantitative analysis further showed that distance from settlements and distance from roads and forest trails are the next most important factors in the occurrence of fires. The correlation coefficients for the functions WSI = f(DS) and WSI = f(DFR) are r = 0.708 and r = 0.608, respectively. Thus, parts of the study area closer to settlements and roads have a higher fire risk. At the same time, these are gentler terrains with smaller slope angles, higher air temperatures, and lower precipitation amounts. The relatively high positive correlation (r = 0.688) between the WSI and WE parameters indicates the importance of wind in assessing fire risk. High TS values correspond to high LU values (r = 0.709). This means that a large part of the study area consists of forests and pastures located on steep terrains. However, regardless of their predisposition to fires, they do not have high WSI values. In this context, the terrain's slope and the land use type did not show significant quantitative agreements with WSI. Similar results were obtained for aspect.

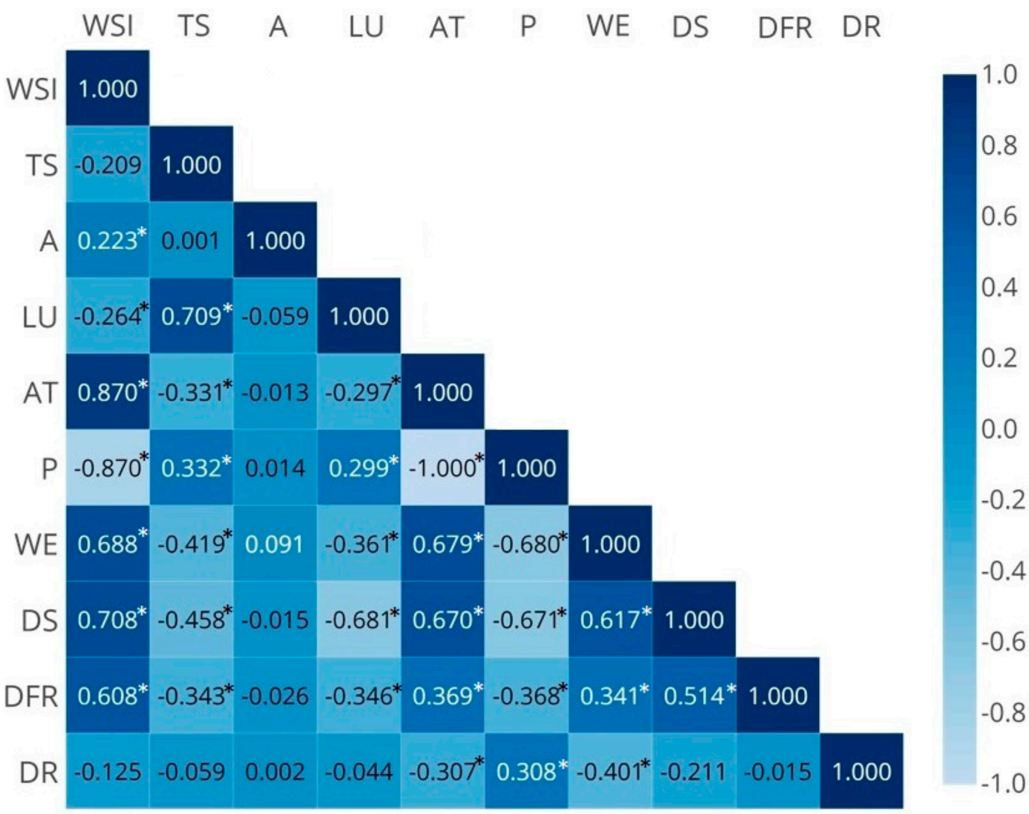

Figure 10. Correlation matrix (Pearson (r)) for parameters for the calculation of the wildfire susceptibility index in the Šar Mountains (significance level α = 0.05; *—significance level α < 0.0001).

4. Discussion

The spatial analysis of the vulnerability of the Šar Mountains National Park to soil erosion and fires has shown that there is no clear correlation between these two hazards (Figures 7 and 8). This is because this study identified the terrain's predisposition for the occurrence of both soil erosion and fires. Thus, areas with a higher risk of fire tend to have a lower potential for intense soil erosion. However, research has shown that post-fire erosion can mobilize large amounts of sediment [92], even with moderate rainfall [93]. Specific changes in the soil and ecosystems after a fire can lead to varying hydrological and erosion responses. In the first years after a fire, soil loss can be significant, and erosion can be intense, especially on slopes. The loss of organic matter reduces soil infiltration, increases surface runoff, alters soil texture and structure, and affects the stability of soil aggregates. Also, slower vegetation recovery can prolong the erosion and runoff process [94]. The impact of wildfire on the landscape usually lasts for about 3 to 4 years, although some effects can persist for as long as 30 years [92]. In recent years, in certain parts of the world, the increasing frequency of fires has led to the highest values of sediment mass and sediment yield [93]. Šar Mountains National Park is characterized by a specific morphometry (large slope angles and high altitude), a high amount of precipitation, and shallow mountain soils. A scarcity of vegetation or complete absence of vegetation after a fire in this area would lead to the occurrence of more intense erosion.

In the context of soil erosion quantification in Serbia, research has shown that even within protected natural areas, surfaces affected by soil erosion can be identified. Despite numerous differences in results, a common feature of all protected areas in Serbia is the small percentage or complete absence of excessive erosion and a large share of areas affected by weak or very weak erosion. This also applies to Šar Mountains National Park.

An analysis of the vulnerability of Fruška Gora National Park to natural hazards showed that 45% of its territory is at risk. The category of intense soil erosion affected 4% of the area, while medium erosion was present in 13% of the area. According to the results of the same research, 8% of the total area of Đerdap National Park was threatened by natural hazards. About 2.5% of the territory was threatened by intense erosion, and 0.2% of the territory was threatened by moderate erosion [28]. Therefore, these results confirm that Šar Mountains National Park is similar to Fruška Gora National Park, particularly in the percentage of medium erosion categories. This erosion category is much smaller in Đerdap National Park. On the other hand, a common characteristic of protected natural areas is their rich forest vegetation. Moreover, protected natural areas are mostly located in border regions, which have specific demographic conditions [63]. This explains the large percentage of weak and very weak erosion categories. In the context of the dynamics of the erosive process, the latest studies show that in 2018, parts of the Landscape of Exceptional Qualities Vlasina were not threatened by stronger categories of erosion, and the intensity of erosive processes had a continuous downward trend [63]. The erosion potential model was used for a comparative assessment of the state of soil erosion across 11 mountain basins in central Serbia for the period of 1971–2010 [95]. Watershed characteristics were divided into five classes, and within each class, 22 variables were calculated: 2 variables related to erosion, 1 to topography, 2 to land cover, 7 to demographics, and 10 agrarian variables. The final results show a decreasing tendency in the intensity of erosion processes in the studied basins.

The protection of natural resources in Serbia does not necessarily mean the absence of anthropogenic activities in these areas. The main dangers to the natural environment are deforestation, soil erosion, illegal and unplanned construction, improper waste disposal, and various forms of pollution, including air, water, and noise [27,96]. Considering the natural predisposition (geological, morphometric, climatic, hydrological) of these areas to various types of hazards, it is not surprising that the protected areas of Serbia show varying levels of vulnerability. A negative example of environmental impact is the construction of a ski resort in Park Nature Stara Planina. The most severe forms of terrain degradation were recorded near Babin Zub. The destruction of native beech forests and meadows led to the creation of anthropogenic bare land, which became the dominant surface in the upper part of the Zubska River watershed. Intensive erosion processes resulted in the formation of furrows and gullies, some reaching depths of up to 3.5 m [97]. This research has shown that there are no such extreme cases in Šar Mountains National Park. Over the past few decades, Kopaonik National Park has been significantly affected by human activities. What was once primarily a naturally protected area has, over time, transformed into the largest ski resort in Serbia. Studies on soil erosion and runoff have revealed that in some parts of the park, agricultural stagnation and population trends have helped to lessen tourism's negative effects [27]. Parts of Zlatibor Nature Park (Poblačnica, Jablanica, and Crni Rzav watersheds) had a similar or even higher intensity of the erosive process (coefficient Z) compared to that in 1990 due to increases in the rural population and agricultural areas [83].

Spatial–temporal patterns of soil erosion intensity in Serbia are most commonly identified using the EPM. However, the study of fire risk in recent years has a much broader methodological framework. This methodological framework includes two directions for the study of fire phenomena. The identification of the degree of danger (spatial patterns of fire occurrence) is one of them.

Of the similar methods for wildfire prediction, the RC index has been developed in Turkey to model wildfires. Erten et al. (2004) used five natural and anthropogenic conditions in their analysis: vegetation, terrain slope, aspect, distance from roads, and distance from settlements [39]. Vegetation was given the highest importance (value 7), while distance from roads and distance from settlements were the least important factors (value 3). In the territory of the Svrljiški Timok Basin, Ćurić et al. [52] used GIS, available data, and the RC index to obtain a map of wildfire vulnerability. A very high level of endangerment was found for 20.81% of the basin area, while 35.73% was highly vulnerable. For the spatial analysis of threat for Golija Nature Park, Novkovic et al. [30] used fuzzy logic, AHP, and the RC index. Very high and high sensitivity zones were recorded over 26.85% of the protected area (according to the RC method). At the same time, the fuzzy AHP approach indicated that 25.75% of the area belonged to the same categories. In recent years, machine learning has become one of the most widely applied approaches for assessing wildfire risk in Serbia. Milanović et al. [45] used two machine learning models—logistic regression (LR) and random forest (RF)—to analyze the territory of eastern Serbia. Their findings revealed that zones with very high fire potential accounted for 19.7% of forest areas using the LR model and 18.9% using the RF model. In this case, the RF model demonstrated better predictive power than LR. Gigović et al. [43] employed ensemble learning, support vector machine (SVM), and RF methods with Bayesian averaging for the Tara National Park area. Their results indicated that the Bayesian average ensemble model delivered the best performance. A study focused on the eastern part of the Šar Mountains, specifically the Sirinić Valley, was conducted by Durlević et al. [29]. They used GIS, remote sensing, and the RC index to assess wildfire susceptibility, revealing that 8.5% of the Sirinić Valley (Štrpce municipality) is very highly susceptible, while 52.4% is highly susceptible to wildfires. Based on these results, Šar Mountains National Park is very similar to Golija Nature Park. Specifically, the category of very high and high fire sensitivity is present in 22% of the study area.

Another direction in the study of fires in Serbia is the study of their dynamics and frequency (number of fires, seasonality, length of fire seasons, influence of climatic conditions on the occurrence of fires, etc.). Živanović et al. [32] investigated the susceptibility of national parks to wildfires in Central Serbia. The results were obtained by applying climate indices (forest aridity index, De Martonne aridity index, and Lang's rain factor) based on air temperature and precipitation for the period of 2005–2021. Spatially, the most frequent fires were within the Tara and Djerdap national parks. The analysis of the temporal dynamics of fires showed that the fire risk was greatest during September and August. Živanović and Tošić [98] studied the susceptibility of Đerdap National Park to forest fires based on three indices (Angstrom index, Nesterov index, and the deficit and surplus of precipitation method) and climatological data from the meteorological station in Veliko Gradište for two time series: 1961–1990 and 1991–2017. The results indicate that the frequency of fires increased in the second climatic period and that June, July, and August were the months with the highest risk of fire occurrence. The Angstrom index and Nesterov index were also used to analyze Tara National Park's vulnerability to wildfires. Lukić et al. [3] investigated causality in the occurrence and frequency of wildfires during the summer days of August and September. The two indices were found to be highly correlated (−0.97), which was expected given that the same meteorological parameters were used in their calculations.

Hence, all of the research papers referenced above emphasize the critical need for implementing integrated methods to monitor and assess areas vulnerable to hydro-meteorological hazards in this region of Southeastern Europe. Given the increasing frequency and severity of such hazards, a comprehensive approach that combines various techniques is essential for accurately identifying high-risk areas, enhancing early warning systems, and developing effective mitigation strategies for risk reduction.

For the adequate protection and planning of the future state of biodiversity, geodiversity, and landscape diversity, it is very important to identify the current state of protected assets. This can be achieved through the creation of multi-hazard maps, which are a crucial initial step in preventing and reducing natural hazards in areas prone to risk [28].

The WSI incorporates nine natural and anthropogenic conditions for which data are readily available in many parts of the world. The wildfire inventory with 365 samples from 2015 to 2024 was used to validate the results (Figure 11). The ROC-AUC method determined a predictive power of 0.71. Although the predictive power is moderate, some differences exist between the wildfire inventory and the WSI methodology. The inventory shows that the majority of fires originate naturally, while the WSI was developed to identify vulnerable areas and potential fires caused by anthropogenic activities. Anthropogenically induced fires have a more destructive environmental impact (residential buildings, roads, industrial complexes, agricultural plots).

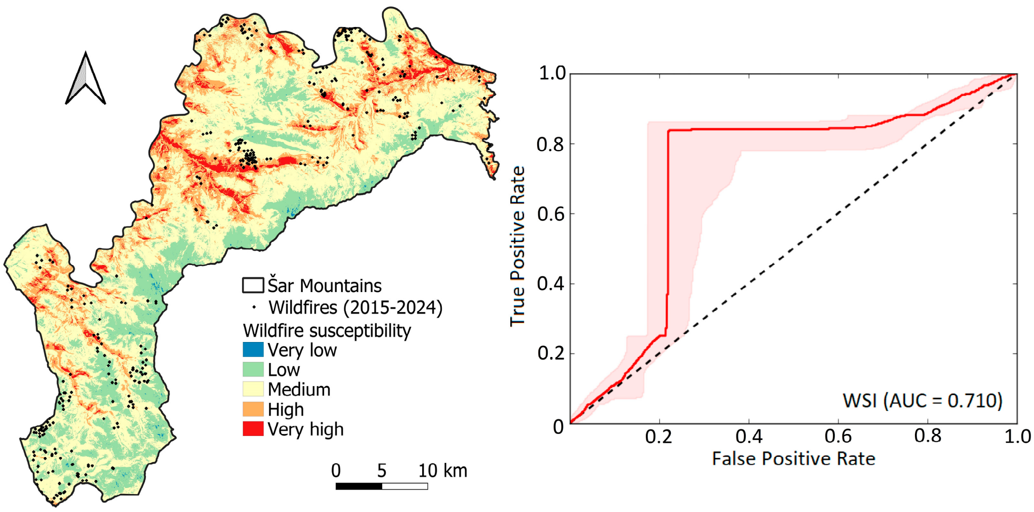

Figure 11. Wildfire inventory and ROC-AUC result validation.

This is the first study to examine the effectiveness of the WSI, but more comprehensive validation of the method requires larger-scale implementation in different climatological regions. As a limitation, the method does not include individual climate parameters (air humidity, wind speed, and direction) that also influence the spatial distribution of wildfires. However, data for these criteria are often micro-localized, not publicly available, and therefore omitted from the WSI. Also, the WSI was developed to model wildfires caused by anthropogenic activity, while the spatial distribution of naturally caused wildfires requires a combination of multiple methodological approaches.

In forest ecosystem management, it is necessary to integrate GIS and remote sensing methods to ensure adequate forest monitoring, determine the intensity of soil erosion susceptibility, and assess the possibility of wildfires [99–120].

5. Conclusions

Soil erosion is a natural process that causes significant forest ecological and economic consequences on the Balkan Peninsula. Wildfires significantly exacerbate this process by removing protective vegetation and increasing soil vulnerability to runoff and sediment loss, linking these two hazards as a critical environmental challenge. At the global level, an increase in erosion intensity is expected due to the increase in the global population, climate extremes, and transformations in land use. In Serbia, the frequency of precipitation has generally increased, so the hydrological cycle has an increasing impact on erosion intensity. In the Šar Mountains, 8.28% of the territory is vulnerable to intense erosion, while excessive erosion is present in 2.17%. These erosion patterns are often amplified in areas recently affected by wildfires, underscoring their interconnected dynamics. The factors that affect the degree of erosion in high mountain areas are mainly physical–geographic. In contrast, agro-geographical factors (roads and land reclamation systems) prevail in settlements and their immediate vicinity. For this reason, it is necessary to implement various erosion protection and mitigation measures depending on the factors that affect erosion intensity and to address the compounding effects of wildfire occurrence.

Zoning areas at risk of forest fires is a crucial first step in implementing preventive measures against wildfires. The vulnerability map provides detailed information on the locations most likely to experience wildfires, and it can be used to optimize the placement of early wildfire detection systems. Special attention is given to protected natural areas due to their biodiversity and increased vulnerability.

Šar Mountains National Park, one of the most significant protected natural areas on the Balkan Peninsula, stands out for its size, biodiversity, and geodiversity. This study developed a wildfire susceptibility index (WSI) to assess the spatial distribution of wildfires. The results of the WSI reveal that 21.3% of the Šar Mountains are highly or very highly susceptible to wildfires. By integrating the EPM with the WSI, this research provides a pioneering dual-hazard assessment framework that concurrently quantifies soil erosion and wildfire susceptibility, offering a comprehensive tool for managing environmental risks in previously unstudied mountainous regions. These findings are essential for effective wildfire risk management, forest management planning, silvicultural practices, ongoing condition monitoring, and the development of early warning systems. This integrated approach emphasizes how wildfire-induced erosion can be predicted and mitigated, enhancing the resilience of fire-prone landscapes. Furthermore, future efforts could leverage this integrated approach to develop a regional predictive model, incorporating real-time climate data and community-based monitoring to enhance proactive hazard mitigation across the Balkan Peninsula. Additionally, the number of wildfires can be reduced through the active involvement of the local community in programs and initiatives informed by a deeper understanding of wildfire dynamics and their role in driving soil erosion.

Author Contributions: Conceptualization, U.D.; methodology, T.S., A.V. and U.D.; software, F.V.; validation, V.D. and U.D.; formal analysis, T.S. and B.A.; investigation, T.L.; resources, B.A.; data curation, A.V.; writing—original draft preparation, U.D.; writing—review and editing, T.L.; visualization, V.D.; supervision, A.V.; project administration, U.D.; funding acquisition, F.V. All authors have read and agreed to the published version of the manuscript.

Funding: This research was funded by the Ministry of Science, Technological Development and Innovation of the Republic of Serbia (Contract number 451-03-136/2025-03/200091).

Data Availability Statement: To obtain the data from this study, please contact the authors via email.

Acknowledgments: The authors are grateful to the anonymous reviewers whose comments and suggestions greatly improved the manuscript.

Conflicts of Interest: The authors declare no conflicts of interest.

References

1. Cremen, G.; Galasso, C.; McCloskey, J. Modelling and quantifying tomorrow's risks from natural hazards. *Sci. Total Environ.* **2022**, *817*, 152552. [CrossRef] [PubMed]
2. Deđanski, V.; Durlević, U.; Kovjanić, A.; Lukić, T. GIS-Based Spatial Modeling of Landslide Susceptibility Using BWM-LSI: A Case Study—City of Smederevo (Serbia). *Open Geosci.* **2024**, *16*, 20220688. [CrossRef]
3. Lukić, T.; Marić, P.; Hrnjak, I.; Gavrilov, M.B.; Mladjan, D.; Zorn, M.; Komac, B.; Milošević, Z.; Marković, S.B.; Sakulski, D.; et al. Forest fire analysis and classification based on Serbian case study. *Acta Geogr. Slov.* **2017**, *57*, 51–63. [CrossRef]
4. Srejić, T.; Manojlović, S.; Sibinović, M.; Bajat, B.; Novković, I.; Milošević, M.V.; Carević, I.; Todosijević, M.; Sedlak, M.G. Agricultural Land Use Changes as a Driving Force of Soil Erosion in the Velika Morava River Basin, Serbia. *Agriculture* **2023**, *13*, 778. [CrossRef]
5. Hou, D.; Bolan, N.; Tsang, D.; Kirkham, M.; O'Connor, D. Sustainable soil use and management: An interdisciplinary and systematic approach. *Sci. Total Environ.* **2020**, *729*, 138961. [CrossRef] [PubMed]
6. Keesstra, S.D.; Bouma, J.; Wallinga, J.; Tittonell, P.; Smith, P.; Cerdà, A.; Montanarella, L.; Quinton, J.; Pachepsky, Y.; Van der Puten, W. The significance of soils and soil science towards realization of the United Nations Sustainable Development Goals. *Soil* **2016**, *2*, 111–128. [CrossRef]
7. Lal, R. Soil erosion and the global carbon budget. *Environ. Int.* **2003**, *29*, 437–450. [CrossRef]
8. Poesen, J. Soil erosion in the Anthropocene: Research needs. *Earth Surf. Process. Landf.* **2018**, *43*, 64–84. [CrossRef]
9. Borrelli, P.; Alewell, C.; Alvarez, P.; Anache, J.; Baartman, J.; Ballabio, C.; Bezak, N.; Biddoccu, M.; Cerda, A.; Chalise, D. Soil erosion modelling: A global review and statistical analysis. *Sci. Total Environ.* **2021**, *780*, 146494. [CrossRef]
10. Di Bene, C.; Francaviglia, R.; Farina, R.; Álvaro-Fuentes, J.; Zornoza, R. Agricultural Diversification. *Agriculture* **2022**, *12*, 369. [CrossRef]
11. Pimentel, D.; Harvey, C.; Resosudarmo, P.; Sinclair, K.; Kurz, D.; Mcnair, M.; Crist, S.; Shpritz, L.; Fitton, L.; Saffouri, R.; et al. Environmental and Economic Costs of Soil Erosion and Conservation Benefits. *Science* **1995**, *267*, 1117–1123. [CrossRef] [PubMed]
12. Altobelli, F.; Vargas, R.; Corti, G.; Dazzi, C.; Montanarella, L.; Monteleone, A.; Caon, L.; Piazza, M.; Calzolari, C.; Munafò, M.; et al. Improving soil and water conservation and ecosystem services by sustainable soil management practices: From a global to an Italian soil partnership. *Ital. J. Agron.* **2020**, *15*, 1765. [CrossRef]
13. Lal, R. Accelerated Soil Erosion as a Source of Atmospheric CO_2. *Soil Till. Res.* **2019**, *188*, 35–40. [CrossRef]
14. Li, Z.Y.; Fang, H.Y. Impacts of Climate Change on Water Erosion: A Review. *Earth Sci. Rev.* **2016**, *163*, 94–117. [CrossRef]
15. Ma, X.; Zhao, C.; Zhu, J. Aggravated Risk of Soil Erosion with Global Warming—A Global Meta-Analysis. *Catena* **2021**, *200*, 105129. [CrossRef]
16. Golosov, V.; Yermolaev, O.; Litvin, L.; Chizhikova, N.; Kiryukhina, Z.; Safina, G. Influence of Climate and Land Use Changes on Recent Trends of Soil Erosion Rates within the Russian Plain. *Land Degrad. Dev.* **2018**, *29*, 2658–2667. [CrossRef]
17. Bento-Gonçalves, A.; Vieira, A.; Santos, S.M.d. Research on Wildfires, Soil Erosion and Land Degradation in the XXI Century. *Fire* **2024**, *7*, 327. [CrossRef]
18. Gavrilović, S. Engineering of Torrents and Erosion. *J. Constr.* **1972**, 1–292. (In Serbian)
19. Tošić, R.; Dragićević, S.; Lovrić, N. Assessment of Soil Erosion and Sediment Yield Changes Using Erosion Potential Model—Case Study: Republic of Srpska (BiH). *CJEES* **2012**, *7*, 147–154.
20. Raza, A.; Ahrends, H.; Habib-Ur-Rahman, M.; Gaiser, T. Modeling Approaches to Assess Soil Erosion by Water at the Field Scale with Special Emphasis on Heterogeneity of Soils and Crops. *Land* **2021**, *10*, 422. [CrossRef]
21. Dragićević, S.; Kostadinov, S.; Novković, I.; Momirović, N.; Langović, M.; Stefanović, T.; Radović, M.; Tošić, R. Assessment of Soil Erosion and Torrential Flood Susceptibility: Case Study—Timok River Basin, Serbia. In *The Lower Danube River: Hydro-Environmental Issues and Sustainability*; Springer International Publishing: Cham, Switzerland, 2022; pp. 357–380. [CrossRef]
22. Polovina, S.; Radić, B.; Ristić, R.; Milčanović, V. Application of Remote Sensing for Identifying Soil Erosion Processes on a Regional Scale: An Innovative Approach to Enhance the Erosion Potential Model. *Remote Sens.* **2024**, *16*, 2390. [CrossRef]
23. Bezak, N.; Borrelli, P.; Mikoš, M.; Jemec Auflič, M.; Panagos, P. Towards Multi-Model Soil Erosion Modelling: An Evaluation of the Erosion Potential Method (EPM) for Global Soil Erosion Assessments. *Catena* **2024**, *234*, 107596. [CrossRef]
24. Dominici, R.; Larosa, S.; Viscomi, A.; Mao, L.; De Rosa, R.; Cianflone, G. Yield Erosion Sediment (YES): A PyQGIS Plug-in for the Sediments Production Calculation Based on the Erosion Potential Method. *Geosciences* **2020**, *10*, 324. [CrossRef]

25. Elaloui, A.; Khalki, E.M.E.; Namous, M.; Ziadi, K.; Eloudi, H.; Faouzi, E.; Bou-Imajjane, L.; Karroum, M.; Tramblay, Y.; Boudhar, A.; et al. Soil Erosion under Future Climate Change Scenarios in a Semi-Arid Region. *Water* **2022**, *15*, 146. [CrossRef]
26. Sakuno, N.R.R.; Guiçardi, A.C.F.; Spalevic, V.; Avanzi, J.C.; Silva, M.L.N.; Mincato, R.L. Adaptation and Application of the Erosion Potential Method for Tropical Soils. *Rev. Ciência Agronômica* **2020**, *51*, e20186545. [CrossRef]
27. Djurdjić, S.; Jakovljević, T. Possibilities and Challenges of Cross-Border Cooperation in the Field of Environmental Protection. In Proceedings of the Tenth Scientific-Professional Meeting with International Participation "Local Self-Government in Planning and Arrangement of Space and Settlements", Pirot, Serbia, 17–19 October 2024; pp. 63–69. (In Serbian).
28. Dragićević, S.; Mészáros, M.; Djurdjić, S.; Pavić, D.; Novković, I.; Tošić, R. Vulnerability of National Parks to Natural Hazards in the Serbian Danube Region. *Pol. J. Environ. Stud.* **2013**, *22*, 1053–1060.
29. Durlević, U.; Novković, I.; Lukić, T.; Valjarević, A.; Samardžić, I.; Krstić, F.; Batoćanin, N.; Mijatov, M.; Ćurić, V. Multihazard Susceptibility Assessment: A Case Study—Municipality of Štrpce (Southern Serbia). *Open Geosci.* **2021**, *13*, 1414–1431. [CrossRef]
30. Novkovic, I.; Marković, G.B.; Lukić, D.; Dragićević, S.; Milošević, M.; Djurdjić, S.; Samardžić, I.; Lezaic, T.; Tadić, M. GIS-Based Forest Fire Susceptibility Zonation with IoT Sensor Network Support, Case Study—Nature Park Golija, Serbia. *Sensors* **2021**, *21*, 6520. [CrossRef]
31. Lukić, D.; Perić, M.; Stankov, S. GIS-AHP Multi Criteria Nature Protection Vulnerability Evaluation Method: A Case Study of Tara National Park, Serbia. *Fresenius Environ. Bull.* **2023**, *32*, 2954–2964.
32. Živanović, S.; Gocić, M.; Tošić, I. Vulnerability of Central Serbian National Parks to Wildfires. *Időjárás* **2024**, *128*, 99–120. [CrossRef]
33. Li, J.; Shan, Y.; Yin, S.; Wang, M.; Sun, L.; Wang, D. Nonparametric Multivariate Analysis of Variance for Affecting Factors on the Extent of Wildfire Damage in Jilin Province, China. *J. For. Res.* **2019**, *30*, 2185–2197. [CrossRef]
34. Zema, D.A.; Nunes, J.P.; Lucas-Borja, M.E. Improvement of Seasonal Runoff and Soil Loss Predictions by the MMF (Morgan-Morgan-Finney) Model after Wildfire and Soil Treatment in Mediterranean Forest Ecosystems. *Catena* **2020**, *188*, 104415. [CrossRef]
35. Das, J.; Mahato, S.; Joshi, P.K.; Liou, Y.-A. Forest Fire Susceptibility Zonation in Eastern India Using Statistical and Weighted Modelling Approaches. *Remote Sens.* **2023**, *15*, 1340. [CrossRef]
36. Bjånes, A.; Fuente, L.D.R.; Mena, P. A Deep Learning Ensemble Model for Wildfire Susceptibility Mapping. *Ecol. Inform.* **2021**, *65*, 101397. [CrossRef]
37. Bahadori, N.; Razavi-Termeh, S.V.; Sadeghi-Niaraki, A.; Al-Kindi, K.M.; Abuhmed, T.; Nazeri, B.; Choi, S.-M. Wildfire Susceptibility Mapping Using Deep Learning Algorithms in Two Satellite Imagery Datasets. *Forests* **2023**, *14*, 1325. [CrossRef]
38. Aleksova, B.; Lukić, T.; Milevski, I.; Puhar, D.; Marković, S.B. Preliminary Assessment of Geohazards' Impacts on Geodiversity in the Kratovska Reka Catchment (North Macedonia). *Geosciences* **2024**, *14*, 62. [CrossRef]
39. Erten, E.; Kurgun, V.; Musaoğlu, N. Forest Fire Risk Zone Mapping from Satellite Imagery and GIS: A Case Study. In Proceedings of the XX Congress of the International Society for Photogrammetry and Remote Sensing, Istanbul, Turkey, 12–23 July 2004; pp. 33–39.
40. Turco, M.; Rosa-Cánovas, J.J.; Bedia, J.; Jerez, S.; Montávez, J.P.; Llasat, M.C.; Provenzale, A. Exacerbated Fires in Mediterranean Europe Due to Anthropogenic Warming Projected with Non-Stationary Climate-Fire Models. *Nat. Commun.* **2018**, *9*, 3821. [CrossRef]
41. Feurdean, A.; Vannière, B.; Finsinger, W.; Warren, D.; Connor, S.C.; Forrest, M.; Liakka, J.; Panait, A.; Werner, C.; Andrič, M.; et al. Fire Hazard Modulation by Long-Term Dynamics in Land Cover and Dominant Forest Type in Eastern and Central Europe. *Biogeosciences* **2020**, *17*, 1213–1230. [CrossRef]
42. Costa, H.; de Rigo, D.; Libertà, G.; Durrant, T.; San-Miguel-Ayanz, J. *European Wildfire Danger and Vulnerability under a Changing Climate: Towards Integrating Risk Dimensions*; EUR 30116 EN; Publications Office of the European Union: Luxembourg, 2020. [CrossRef]
43. Gigović, L.; Pourghasemi, H.R.; Drobnjak, S.; Bai, S. Testing a New Ensemble Model Based on SVM and Random Forest in Forest Fire Susceptibility Assessment and Its Mapping in Serbia's Tara National Park. *Forests* **2019**, *10*, 408. [CrossRef]
44. Thuiller, W.; Lavorel, S.; Araújo, M.B.; Sykes, M.T. Climate Change Threats to Plant Diversity in Europe. *Proc. Natl. Acad. Sci. USA* **2005**, *102*, 8245–8250. [CrossRef]
45. Milanović, S.; Marković, N.; Pamučar, D.; Gigović, L.; Kostić, P.; Milanović, S.D. Forest Fire Probability Mapping in Eastern Serbia: Logistic Regression versus Random Forest Method. *Forests* **2021**, *12*, 5. [CrossRef]
46. Demir, A.; Akay, A.E. Forest Fire Risk Mapping Using GIS-Based Analytical Hierarchy Process Approach. *Eur. J. For. Eng.* **2024**, *10*, 15–28. [CrossRef]
47. Dong, X.; Li-min, D.; Guo-fan, S.; Lei, T.; Hui, W. Forest Fire Risk Zone Mapping from Satellite Images and GIS for Baihe Forestry Bureau, Jilin, China. *J. For. Res.* **2005**, *16*, 169–174. [CrossRef]
48. Tiwari, A.; Shoab, M.; Dixit, A. GIS-Based Forest Fire Susceptibility Modeling in Pauri Garhwal, India: A Comparative Assessment of Frequency Ratio, Analytic Hierarchy Process and Fuzzy Modeling Techniques. *Nat. Hazards* **2021**, *105*, 1189–1230. [CrossRef]

49. Pourghasemi, H.R.; Beheshtirad, M.; Pradhan, B. A Comparative Assessment of Prediction Capabilities of Modified Analytical Hierarchy Process (M-AHP) and Mamdani Fuzzy Logic Models using Netcad-GIS for Forest Fire Susceptibility Mapping. *Geomat. Nat. Hazards Risk* **2016**, *7*, 861–885. [CrossRef]
50. QGIS Development Team. QGIS Geographic Information System v3.28.10 with GRASS. Open Source Geospatial Foundation Project. 2023. Available online: http://qgis.osgeo.org (accessed on 18 June 2023).
51. Nikolić, G.; Vujović, F.; Golijanin, J.; Šiljeg, A.; Valjarević, A. Modelling of Wildfire Susceptibility in Different Climate Zones in Montenegro Using GIS-MCDA. *Atmosphere* **2023**, *14*, 929. [CrossRef]
52. Ćurić, V.; Durlević, U.; Ristić, N.; Novković, I.; Čegar, N. GIS Application in Analysis of Threat of Forest Fires and Landslides in the Svrljiški Timok Basin (Serbia). *Bull. Serbian Geograph. Soc.* **2022**, *102*, 107–130. [CrossRef]
53. Durlević, U.; Novković, I.; Bajić, S.; Milinčić, M.; Valjarević, A.; Čegar, N.; Lukić, T. Snow Avalanche Hazard Prediction Using the Best-Worst Method—Case Study: The Šar Mountains, Serbia. In *Advances in Best-Worst Method*; Rezaei, J., Brunelli, M., Mohammadi, M., Eds.; Springer: Cham, Switzerland, 2023; pp. 211–216. [CrossRef]
54. Stojković, S.; Marković, D.; Durlević, U. Snow Cover Estimation Using Sentinel-2 High Spatial Resolution Data: A Case Study: National Park Šar Planina (Serbia). In *Advanced Technologies, Systems, and Applications VII*; Ademović, N., Mujčić, E., Mulić, M., Kevrić, J., Akšamija, Z., Eds.; Springer: Cham, Switzerland, 2023; pp. 507–519. [CrossRef]
55. Durlević, U.; Valjarević, A.; Novković, I.; Ćurčić, N.B.; Smiljić, M.; Morar, C.; Stoica, A.; Barišić, D.; Lukić, T. GIS-Based Spatial Modeling of Snow Avalanches Using Analytic Hierarchy Process: A Case Study of the Šar Mountains, Serbia. *Atmosphere* **2022**, *13*, 1229. [CrossRef]
56. Institute of Nature Conservation of Serbia. Protected Areas, National Park Šar Planina. 2024. Available online: https://zzps.rs (accessed on 23 February 2024).
57. Durlević, U.; Valjarević, A.; Novković, I.; Vujović, F.; Josifov, N.; Krušić, J.; Komac, B.; Đekić, T.; Singh, S.K.; Jović, G.; et al. Universal Snow Avalanche Modeling Index Based on SAFI–Flow-R Approach in Poorly-Gauged Regions. *ISPRS Int. J. Geo-Inf.* **2024**, *13*, 315. [CrossRef]
58. Aleksova, B.; Milevski, I.; Dragićević, S.; Lukić, T. GIS-Based Integrated Multi-Hazard Vulnerability Assessment in Makedonska Kamenica Municipality, North Macedonia. *Atmosphere* **2024**, *15*, 774. [CrossRef]
59. Tošić, R.; Dragićević, S. *Chronological Development of the Erosion Potential Method*; Serbian Geographical Society: Belgrade, Serbia, 2024. (In Serbian)
60. Geoliss. Basic Geological Map of Former Yugoslavia. 1979. Available online: https://geoliss.mre.gov.rs/prez/OGK/RasterSrbija/ (accessed on 9 February 2024).
61. Environmental Systems Research Institute [ESRI]. Sentinel-2 Land Cover Explorer. 2023. Available online: https://livingatlas.arcgis.com/landcoverexplorer/#mapCenter=21.076,42.197,13&mode=step&timeExtent=2017,2023&year=2023 (accessed on 12 February 2024).
62. Stefanidis, S.; Mallinis, G.; Alexandridis, V. Multi-Decadal Monitoring of Soil Erosion Rates in South Europe. *Environ. Sci. Proc.* **2023**, *26*, 138. [CrossRef]
63. Durlević, U.; Momčilović, A.; Ćurić, V.; Dragojević, M. GIS Application in Analysis of Erosion Intensity in the Vlasina River Basin. *Bull. Serbian Geograph. Soc.* **2019**, *99*, 17–36. [CrossRef]
64. Sivrikaya, F.; Sağlam, B.; Akay, A.E.; Bozali, N. Evaluation of Forest Fire Risk with GIS. *Pol. J. Environ. Stud.* **2014**, *23*, 187–194.
65. Alaska Satellite Facility. ALOS PALSAR. 2006. Available online: https://search.asf.alaska.edu/#/ (accessed on 10 February 2024).
66. Nguyen, C.T.; Chidthaisong, A.; Kieu Diem, P.; Huo, L.-Z. A Modified Bare Soil Index to Identify Bare Land Features During Agricultural Fallow-Period in Southeast Asia Using Landsat 8. *Land* **2021**, *10*, 231. [CrossRef]
67. Diek, S.; Fornallaz, F.; Schaepman, M.; De Jong, R. Barest Pixel Composite for Agricultural Areas Using Landsat Time Series. *Remote Sens.* **2017**, *9*, 1245. [CrossRef]
68. Iban, M.C.; Aksu, O. SHAP-Driven Explainable Artificial Intelligence Framework for Wildfire Susceptibility Mapping Using MODIS Active Fire Pixels: An In-Depth Interpretation of Contributing Factors in Izmir, Türkiye. *Remote Sens.* **2024**, *16*, 2842. [CrossRef]
69. Živanović, S.; Gocić, M. Forest Fires in Serbia—Influence of Humidity Conditions. *J. Geogr. Inst. Cvijic* **2022**, *72*, 221–228. [CrossRef]
70. Yu, Q.; Zhao, Y.; Yin, Z.; Xu, Z. Wildfire Susceptibility Prediction Based on a CA-Based CCNN with Active Learning Optimization. *Fire* **2024**, *7*, 201. [CrossRef]
71. Rozas, H.; Xie, W.; Gebraeel, N. Condition-Based Maintenance for Wind Farms Using a Distributionally Robust Chance Constrained Program. *IEEE Trans. Power Syst.* **2025**, *40*, 231–243. [CrossRef]
72. Abouali, A.; Viegas, X.D.; Raposo, R.J. Analysis of the Wind Flow and Fire Spread Dynamics over a Sloped–Ridgeline Hill. *Combust. Flame* **2021**, *234*, 111724. [CrossRef]
73. Francos, M.; Colino-Prieto, F.; Sánchez-García, C. How Mediterranean Ecosystem Deals with Wildfire Impact on Soil Ecosystem Services and Functions: A Review. *Land* **2024**, *13*, 407. [CrossRef]

74. Florath, J.; Chanussot, J.; Keller, S. Road Accessibility during Natural Hazards Based on Volunteered Geographic Information Data and Network Analysis. *ISPRS Int. J. Geo-Inf.* **2024**, *13*, 107. [CrossRef]
75. Open Street Map. Data Export. 2023. Available online: https://www.openstreetmap.org/export#map=4/48.89/29 (accessed on 25 June 2023).
76. Yue, W.; Ren, C.; Liang, Y.; Liang, J.; Lin, X.; Yin, A.; Wei, Z. Assessment of Wildfire Susceptibility and Wildfire Threats to Ecological Environment and Urban Development Based on GIS and Multi-Source Data: A Case Study of Guilin, China. *Remote Sens.* **2023**, *15*, 2659. [CrossRef]
77. Dai, T.; Wang, L.; Li, T.; Qiu, P.; Wang, J. Study on the Characteristics of Soil Erosion in the Black Soil Area of Northeast China under Natural Rainfall Conditions: The Case of Sunjiagou Small Watershed. *Sustainability* **2022**, *14*, 8284. [CrossRef]
78. Baharvand, S.; Pradhan, B. Erosion and Flood Susceptibility Evaluation in a Catchment of Kopet-Dagh Mountains Using EPM and RFM in GIS. *Environ. Earth Sci.* **2022**, *81*, 490. [CrossRef]
79. Salma, K.; Ahmed, A.; Abdellah, A.; Salma, E. Estimation and mapping of water erosion and soil loss: Application of Gavrilovic erosion potential model (EPM) using GIS and remote sensing in the Assif el mal Watershed, Western high Atlas. *China Geol.* **2024**, *7*, 672–685. [CrossRef]
80. Lazarević, R. Erosion in Serbia. *Belgrade Želnid* **2009**, 1–294. (In Serbian)
81. Milevski, I.; Aleksova, B.; Lukić, T.; Dragićević, S.; Valjarević, A. Multi-Hazard Modeling of Erosion and Landslide Susceptibility at the National Scale in the Example of North Macedonia. *Open Geosci.* **2024**, *16*, 20220718. [CrossRef]
82. Kostadinov, S.; Braunović, S.; Dragićević, S.; Zlatić, M.; Dragović, N.; Rakonjac, N. Effects of Erosion Control Works: Case Study—Grdelica Gorge, the South Morava River (Serbia). *Water* **2018**, *10*, 1094. [CrossRef]
83. Petrović, A.M.; Manojlović, S.; Srejić, T.; Zlatanović, N. Insights into Land-Use and Demographical Changes: Runoff and Erosion Modifications in the Highlands of Serbia. *Land* **2024**, *13*, 1342. [CrossRef]
84. Ouallali, A.; Kader, S.; Bammou, Y.; Aqnouy, M.; Courba, S.; Beroho, M.; Briak, H.; Spalevic, V.; Kuriqi, A.; Hysa, A. Assessment of the Erosion and Outflow Intensity in the Rif Region under Different Land Use and Land Cover Scenarios. *Land* **2024**, *13*, 141. [CrossRef]
85. Srejić, T.; Manojlović, S.; Kričković, E. Spatial Differentiation of the Intensity of Soil Erosion According to Predominant Geographical Factors in the Municipality of Rekovac. In *Proceedings—VI Congress of Geographers of Serbia with International Participation*; University of Belgrade: Belgrade, Serbia, 2024; pp. 103–111. (In Serbian)
86. Manojlović, S. *Influence of Geographical Factors on Changes in the Intensity of Water Erosion in the Nišava River Basin*; University of Belgrade, Faculty of Geography: Belgrade, Serbia, 2019. (In Serbian)
87. Elbadaoui, K.; Mansour, S.; Ikirri, M.; Abdelrahman, K.; Abu-Alam, T.; Abioui, M. Integrating Erosion Potential Model (EPM) and PAP/RAC Guidelines for Water Erosion Mapping and Detection of Vulnerable Areas in the Toudgha River Watershed of the Central High Atlas, Morocco. *Land* **2023**, *12*, 837. [CrossRef]
88. Yesuph, A.Y.; Dagnew, A.B. Soil Erosion Mapping and Severity Analysis Based on RUSLE Model and Local Perception in the Beshillo Catchment of the Blue Nile Basin, Ethiopia. *Environ. Syst. Res.* **2019**, *8*, 17. [CrossRef]
89. Attoubounou, R.A.; Diawara, H.; Ludwig, R.; Adounkpe, J. Quantification of Soil–Water Erosion Using the RUSLE Method in the Mékrou Watershed (Middle Niger River). *ISPRS Int. J. Geo-Inf.* **2025**, *14*, 28. [CrossRef]
90. Fire Information for Resource Management System [FIRMS]. Archive Download. 2025. Available online: https://firms.modaps.eosdis.nasa.gov/download/ (accessed on 15 February 2025).
91. Dragićević, S.; Pripužić, M.; Živković, N.; Novković, I.; Kostadinov, S.; Langović, M.; Milojković, B.; Čvorović, Z. Spatial and Temporal Variability of Bank Erosion during the Period 1930–2016: Case Study—Kolubara River Basin (Serbia). *Water* **2017**, *9*, 748. [CrossRef]
92. Santi, P.M.; Rengers, F.K. 9.32—Wildfire and Landscape Change. In *Treatise on Geomorphology*, 2nd ed.; Jack, J., Shroder, F., Eds.; Academic Press: San Diego, CA, USA, 2022; pp. 765–797.
93. Dow, H.W.; East, A.E.; Sankey, J.B.; Warrick, J.A.; Kostelnik, J.; Lindsay, D.N.; Kean, J.W. Postfire sediment mobilization and its downstream implications across California, 1984–2021. *J. Geophys. Res. Earth Surf.* **2024**, *129*, e2024JF007725. [CrossRef]
94. Shakesby, R. Post-wildfire soil erosion in the Mediterranean: Review and future research directions. *Earth Sci. Rev.* **2011**, *105*, 71–100. [CrossRef]
95. Manojlović, S.; Sibinović, M.; Srejić, T.; Novković, I.; Milošević, M.V.; Gatarić, D.; Carević, I.; Batoćanin, N. Factors Controlling the Change of Soil Erosion Intensity in Mountain Watersheds in Serbia. *Front. Environ. Sci.* **2022**, *10*, 888901. [CrossRef]
96. Potić, I.M.; Ćurčić, N.B.; Radovanović, M.M.; Stanojević, G.B.; Malinović-Milićević, S.B.; Yamashkin, S.A.; Yamashkin, A.A. Estimation of Soil Erosion Dynamics Using Remote Sensing and SWAT in Kopaonik National Park, Serbia. *J. Geogr. Inst. Cvijic* **2021**, *71*, 231–247. [CrossRef]
97. Ristić, R.; Vasiljević, N.; Radić, B.; Radivojević, S. Degradation of Landscape in Serbian Ski Resorts: Aspects of Scale and Transfer of Impacts. *SPATIUM Int. Rev.* **2009**, *20*, 49–52. [CrossRef]

98. Živanović, S.; Tošić, I. Influence of Climatic Conditions on Fire Risk in Djerdap National Park (Serbia): A Case Study of September 2011. *Therm. Sci.* **2020**, *24*, 2845–2855. [CrossRef]
99. Malušević, I.; Ristić, R.; Radić, B.; Polovina, S.; Milčanović, V.; Nešković, P. A Historical Overview of Methods for the Estimation of Erosion Processes on the Territory of the Republic of Serbia. *Land* **2025**, *14*, 405. [CrossRef]
100. Alsaihani, M.; Alharbi, R. Mapping of Soil Erosion Vulnerability in Wadi Bin Abdullah, Saudi Arabia through RUSLE and Remote Sensing. *Water* **2024**, *16*, 2663. [CrossRef]
101. Nieto, C.E.; Martínez-Graña, A.M.; Merchán, L. Soil Erosion Risk Analysis in the Ría de Arosa (Pontevedra, Spain) Using the RUSLE and GIS Techniques. *Forests* **2024**, *15*, 1481. [CrossRef]
102. Erdoğan Yüksel, E.; Karan, Ö.F.; Akay, A.E. Spatio-Temporal Analysis of Erosion Risk Assessment Using GIS-Based AHP Method: A Case Study of Doğancı Dam Watershed in Bursa (Türkiye). *Forests* **2024**, *15*, 1135. [CrossRef]
103. Bao, M.; Liu, J.; Ren, H.; Liu, S.; Ren, C.; Chen, C.; Liu, J. Research Trends in Wildland Fire Prediction Amidst Climate Change: A Comprehensive Bibliometric Analysis. *Forests* **2024**, *15*, 1197. [CrossRef]
104. Zhang, T.; Wang, D.; Lu, Y. A Dynamic Spatiotemporal Understanding of Changes in Social Vulnerability to Wildfires at Local Scale. *Fire* **2024**, *7*, 251. [CrossRef]
105. Shin, S.S.; Park, S.D.; Kim, G. Applicability Comparison of GIS-Based RUSLE and SEMMA for Risk Assessment of Soil Erosion in Wildfire Watersheds. *Remote Sens.* **2024**, *16*, 932. [CrossRef]
106. Radovanović, M.; Pereira Gomes, J.F.; Yamashkin, A.A.; Milenković, M.; Stevančević, M. Electrons or Protons: What Is the Cause of Forest Fires in Western Europe on June 18, 2017? *J. Geogr. Inst. "Jovan Cvijić" SASA* **2017**, *67*, 213–218. [CrossRef]
107. Čupić, A.; Smičiklas, I.; Manić, M.; Đokić, M.; Dragović, R.; Đorđević, M.; Gocić, M.; Jović, M.; Topalović, D.; Gajić, B.; et al. ^{137}Cs-Based Assessment of Soil Erosion Rates in a Morphologically Diverse Catchment with Varying Soil Types and Vegetation Cover: Relationship with Soil Properties and RUSLE Model Predictions. *Water* **2025**, *17*, 526. [CrossRef]
108. Nur, A.S.; Kim, Y.J.; Lee, J.H.; Lee, C.-W. Spatial Prediction of Wildfire Susceptibility Using Hybrid Machine Learning Models Based on Support Vector Regression in Sydney, Australia. *Remote Sens.* **2023**, *15*, 760. [CrossRef]
109. Milenković, M.; Ducić, V.; Obradović, D.; Dedić, A.; Burić, D. Climatic and Anthropogenic Impacts on Forest Fires in Conditions of Extreme Fire Danger on Sandy Soils. *J. Geogr. Inst. "Jovan Cvijić" SASA* **2023**, *73*, 155–168. [CrossRef]
110. Falaras, T.; Tselka, I.; Papadopoulos, I.; Nikolidaki, M.; Karavias, A.; Bafi, D.; Petani, A.; Krassakis, P.; Parcharidis, I. Operational Mapping and Post-Disaster Hazard Assessment by the Development of a Multiparametric Web App Using Geospatial Technologies and Data: Attica Region 2021 Wildfires (Greece). *Appl. Sci.* **2022**, *12*, 7256. [CrossRef]
111. Đokić, M.; Manić, M.; Đorđević, M.; Gocić, M.; Čupić, A.; Jović, M.; Dragović, R.; Gajić, B.; Smičiklas, I.; Dragović, S. Remote Sensing and Nuclear Techniques for High-Resolution Mapping and Quantification of Gully Erosion in the Highly Erodible Area of the Malčanska River Basin, Eastern Serbia. *Environ. Res.* **2023**, *235*, 116679. [CrossRef] [PubMed]
112. Manić, M.; Đorđević, M.; Đokić, M.; Dragović, R.; Kićović, D.; Đorđević, D.; Jović, M.; Smičiklas, I.; Dragović, S. Remote Sensing and Nuclear Techniques for Soil Erosion Research in Forest Areas: Case Study of the Crveni Potok Catchment. *Front. Environ. Sci.* **2022**, *10*, 897248. [CrossRef]
113. González, F.; Morante-Carballo, F.; González, A.; Bravo-Montero, L.; Benavidez-Silva, C.; Tedim, F. Assessment of Forest Fire Severity for a Management Conceptual Model: Case Study in Vilcabamba, Ecuador. *Forests* **2024**, *15*, 2210. [CrossRef]
114. Shin, S.S.; Park, S.D.; Kim, G. Risk Assessment of Soil Erosion Using a GIS-Based SEMMA in Post-Fire and Managed Watershed. *Sustainability* **2022**, *14*, 7339. [CrossRef]
115. Dosis, S.; Petropoulos, G.P.; Kalogeropoulos, K. A Geospatial Approach to Identify and Evaluate Ecological Restoration Sites in Post-Fire Landscapes. *Land* **2023**, *12*, 2183. [CrossRef]
116. Li, Y.; Wu, G.; Zhang, S.; Li, M.; Nie, B.; Chen, Z. A Novel Method of Modeling Grassland Wildfire Dynamics Based on Cellular Automata: A Case Study in Inner Mongolia, China. *ISPRS Int. J. Geo-Inf.* **2023**, *12*, 474. [CrossRef]
117. Tzouveleki, M.; Hatzaki, M.; Antoniou, V.; Karali, A.; Giannakopoulos, C. Modelling Future Forest Fire Risk for the Tourism Sector of Crete. *Environ. Sci. Proc.* **2023**, *26*, 150. [CrossRef]
118. Jo, H.-W.; Krasovskiy, A.; Hong, M.; Corning, S.; Kim, W.; Kraxner, F.; Lee, W.-K. Modeling Historical and Future Forest Fires in South Korea: The FLAM Optimization Approach. *Remote Sens.* **2023**, *15*, 1446. [CrossRef]
119. Asensio, M.I.; Cascón, J.M.; Prieto-Herráez, D.; Ferragut, L. An Historical Review of the Simplified Physical Fire Spread Model PhyFire: Model and Numerical Methods. *Appl. Sci.* **2023**, *13*, 2035. [CrossRef]
120. Tonini, M.; Pereira, M.G.; Fiorucci, P. Performance and Efficiency of Machine Learning Based Approaches for Wildfire Susceptibility Mapping. *Environ. Sci. Proc.* **2022**, *17*, 38. [CrossRef]